Talanta 83 (2010) 178–184

Contents lists available at ScienceDirect

Talanta

journal homepage: www.elsevier.com/locate/talanta

High resolution detection of high mass proteins up to 80,000 Da via multifunctional CdS quantum dots in laser desorption/ionization mass spectrometry

Yaotang Ke [a], Suresh Kumar Kailasa [a,b], Hui-Fen Wu [a,b,c,*], Zhen-Yu Chen [a]

[a] Department of Chemistry, National Sun Yat-Sen University, Kaohsiung 80424, Taiwan
[b] Center for Nanoscience and Nanotechnology, National Sun Yat-Sen University, Kaohsiung 80424, Taiwan
[c] Doctoral Degree Program in Marine Biotechnology, National Sun Yat-Sen University, Kaohsiung 80424, Taiwan

ARTICLE INFO

Article history:
Received 12 July 2010
Received in revised form 1 September 2010
Accepted 3 September 2010
Available online 15 September 2010

Keywords:
CdS quantum dots
Peptides
Proteins
SEM
TEM
MALDI-TOF-MS

ABSTRACT

CdS quantum dots (~5 nm) are used as multifunctional nanoprobes as an effective matrix for large proteins, peptides and as affinity probes for the enrichment of tryptic digest proteins (lysozyme, myoglobin and cytochrome *c*) in laser desorption/ionization time-of-flight mass spectrometry (LDI-TOF MS). The use of CdS quantum dots (CdS QDs) as the matrix allows acquisition of high resolution LDI mass spectra for large proteins (5000–80,000 Da). The enhancement of mass resolution is especially notable for large proteins such as BSA, HSA and transferrin (34–49 times) when compared with those obtained by using SA as the matrix. This technique demonstrates the potentiality of LDI-TOF-MS as an appropriate analytical tool for the analysis of high-molecular-weight biomolecules with high mass resolution. In addition, CdS QDs are also used as matrices for background-free detection of small biomolecules (peptides) and as affinity probes for the enrichment of tryptic digest proteins in LDI-TOF-MS.

1. Introduction

Nanomaterials have exhibited promising potential applications in interdisciplinary and multidisciplinary science [1–3]. Nanomaterials have unique and fascinating physicochemical properties which make them a significant impact in nanobioscience research [4,5]. Importantly, QDs have capability for real-time observations of ligand–receptor interactions which provide for the ultrasensitive detection of biomolecules at single-dot-level [6]. Nanomaterial-based mass spectrometry has received great attention in multidisciplinary science since its introduction by Tanaka's and Karas's groups [7,8]. It is capable for rapid identification of large biomolecules with high sensitivity [9–12]. Conventionally, aromatic acids or aromatic carbonyl compounds were used as the matrices in the LDI-MS, which was termed as matrix assisted laser desorption/ionization mass spectrometry (MALDI-TOF-MS). However, problems can arise when using organic matrices in the MALDI-TOF-MS. For example, low resolution mass spectra for large proteins (MW > 5000 Da) and high interference at low-mass region (MW < 600 Da) limiting its efficiency for high-throughput analysis [13]. Therefore, in the recent years, great efforts have been made on the utilization of nanoparticles (NPs) as assisted matrices in LDI-TOF-MS for efficient biomolecule analysis with reduced background interferences [13].

To date, several nanomaterials including silicon materials [14,15], carbon-based polymers [16,17], magnetic NPs [18], gold NPs [19,20] and TiO_2 NPs [21] have been used as effective matrices for the analysis of biomolecules in MALDI-TOF-MS. Very recently, Girault and co-workers have developed TiO_2 printed aluminum foil as a target plate for laser desorption/ionization of peptides [22]. In continuation, the same group developed photoelectrode array and photosensitive TiO_2 nanomaterial target plates by photocatalytic redox reactions for efficient analysis of peptide fragments in LDI-MS [23,24]. Russell and co-workers analyzed the biomolecules with increased ion yields using size-selective gold NPs as matrices in LDI-MS [20,25]. Later, the same group used Ag NPs (20 and 60 nm) as the matrix for the selective ionization of olefinic compounds in LDI-MS [26]. Chen and co-workers developed titania nanotube arrays and used Fe_3O_4 NPs as matrices for the analysis of various proteins [27]. Therefore, NPs-based mass spectrometry is exceptionally well suited for desorption/ionization of biomolecules in the LDI-MS with various degrees of success. However, so far, NPs-based mass spectrometry has limited ability to ionize larger proteins with high mass resolution.

* Corresponding author at: Department of Chemistry, National Sun Yat-Sen University, Kaohsiung 80424, Taiwan. Tel.: +886 7 5252000/3955; fax: +866 7 5253908..
E-mail address: hwu@faculty.nsysu.edu.tw (H.-F. Wu).

0039-9140/$ – see front matter © 2010 Elsevier B.V. All rights reserved.
doi:10.1016/j.talanta.2010.09.003

In the present study, we have applied CdS QDs modified with 3-mercaptopropanoic acid as an effective matrix for the desorption/ionization of large proteins (insulin, riboneclease A, trypsin, trypsinogen, BSA, HSA and transferrin) with high resolution in a linear MALDI-TOF-MS. We also used CdS QDs as the matrix for background-free detection of small molecules (peptides). In addition, the CdS QDs efficiently could also act as affinity probes for enrichment of tryptic digested proteins (lysozyme, myoglobin and cytochrome *c*).

2. Experimental

2.1. Chemicals

Cadmium nitrate tetrahydrate, 3-mercaptopropionic acid (MPA) were purchased from Fluka (Buchs, Switzerland). Sodium sulfide nonahydrate was obtained from Nihow Shiyak Industries Ltd., Japan. 2,5-Dihydroxybenzoic acid (2,5-DHB) and 3,5-dimethoxy-4-hydroxycinnamic acid (SA) (Alfa Aesar, Lancaster) were obtained from Riedel-de Haën (Seelze, Germany). Insulin, ribonuclease A, trypsin, trypsinogen, apo-transferrin (human), albumin from human serum (HSA), albumin from bovine serum (BSA), bradykinin fragment (1–8), gramicidin D, substance P and ammonium hydroxide were obtained from Sigma–Aldrich (St. Louis, MO, USA). Acetonitrile, hydrochloric acid and trifluoroacetic acid (TFA) were purchased from Wako Pure Chemicals (Osaka, Japan). The water was purified by using Milli-Q system (Millipore, Bedford, MA, USA).

2.2. Solutions

Stock solution of insulin was prepared by dissolving (mg/mL) in deionized water. Stock solutions of myoglobin, lysozyme, cytochrome *c*, ribonuclease A, trypsin, trypsinogen, BSA, HSA, and transferrin were prepared in (mg/mL) 50 mM of NH_4HCO_3 solution. Stock solutions of peptides of gramicidin D, bradykinin fragment (1–8) and substance P were prepared (mg/mL) in methanol. 0.133 M of SA and 2,5-DHB (20 mg/mL) were prepared in 2:1 mixture of acetonitrile–water containing 0.1% of trifluoroacetic acid (TFA). The safety concerns were maintained while doing the experiments and handling of proteins, peptides, organic solvents and chemicals.

2.3. Synthesis of CdS quantum dots

400 μL of 3-MPA was transferred into a 250 mL round bottom flask containing 15 mL of deionized water. To this, 2 mL of 0.01 M cadmium nitrate solution was added drop wise under N_2 pressure with constant stirring for 1 h. The pH of the solution was adjusted to 9 by adding ammonium hydroxide solution. 2.5 ml of 0.008 M sodium sulphide solution was quickly added to the above solution at 96 °C and solution was stirred for 2 h. The obtained clean green-yellowish CdS QDs solution was stored at 4 °C until further use.

2.4. Procedure for the preparation of nanoprobes

750 μL of standard solution of analytes (proteins or peptides) was taken into a 1 mL polyethylene vial. 250 μL of known concentration of CdS QDs solution was added and pH of the test solution was controlled by adding 0.1 M HCl or NaOH. The sample vials were vortexed for 30 min at 900 rpm and then 1 μL of the above test solution was placed on the target plates for MALDI-TOF-MS analysis.

2.5. Procedure for the tryptic digestion of proteins

Protein solutions such as lysozyme (6.9×10^{-5} M), myoglobin (5.8×10^{-5} M), cytochrome *c* (8.0×10^{-5} M) and trypsin (4.0×10^{-5} M) were diluted with 25 mM of NH_4HCO_3 solution containing 8 M of urea and incubated for 30 min. To the above protein solutions, 20 μL of 50 mM dithiothreitol was added and incubated for 1 h at 37 °C to reduce disulfide linkage of protein. After that, the mixture was diluted with 50 mM of NH_4HCO_3 (10-fold) and 40 μL of trypsin solution was added. The protease:protein ratio was maintained at 1:40 *(w/w)* to produce proteolytic digests. The samples were incubated at room temperature for 24 h. Finally, 1 μL of 1% TFA containing ACN:H_2O 1:2 *(v/v)* was added to stop the proteolytic digestion.

2.6. Procedure for the enrichment of tryptic digest proteins

5 μL of the tryptic digested protein samples (myoglobin, lysozyme and cytochrome *c*) were mixed with 0.20% of TFA containing ACN:H_2O 1:2 *(v/v)* and then diluted (10-folds) with buffer solution. To this, 20 μL of CdS QDs solution was added and incubated for 30 min. The solution of CdS QD-conjugated tryptic digest proteins was centrifuged at 18,000 rpm for 2 min. The upper layer was removed and then 0.5 μL of 2,5-DHB solution (20 mg/mL) was added and mixed well. The CdS QD-conjugated tryptic digest proteins with 2,5-DHB solution (0.5 μL) was deposited on the target plate and then analyzed by MALDI-TOF-MS. Figure S1a and b of Supporting Information describes the schematic procedure of CdS QDs as the matrix and as affinity probes for the analysis of proteins and peptides in LDI-TOF-MS.

2.7. Instrumentation

High resolution-transmission electron microscope (HR-TEM) images were obtained using a JEOL TEM-3010 (Tokyo, Japan) at 75 keV. Scanning electron microscope (SEM) images were acquired using a JOEL 6700F, Japan. A 100 Fourier transform infrared (FT-IR) spectrophotometer (PerkinElmer, Boston, MA) and a double-beam spectrophotometer (U3501, Hitachi, Tokyo, Japan) were used for the characterization of CdS QDs. All mass spectra were obtained at positive ion mode using Microflex (Bruker Daltonics, Bremen, Germany) time-of-flight mass spectrometer. 337 nm nitrogen laser was used for irradiation of the sample and other parameters are the same as described in our previous paper [28].

3. Results and discussion

3.1. Spectral characteristics of CdS QDs

Figure S2 of Supporting Information shows UV–vis absorption and fluorescence emission spectra of CdS QDs capped with 3-MPA. The maximum absorption wavelength was observed at 397 nm. The strong (orange) emission peak was observed at 620 nm; indicating that the 3-MPA was successfully attached onto the surfaces of CdS QDs and these results are agreed with the literature [29]. Successful surface modification of CdS QDs with MPA was verified by FT-IR. Figure S3 of Supporting Information shows that the FT-IR spectrum of functionalized CdS QDs with 3-MPA. The strong stretching band for –C=O of mercaptocarboxylic group was observed at 1716 cm^{-1}. The weak bending band of aliphatic C–H group appeared at 1417 cm^{-1}. The stretching vibrations of symmetric and antisymmetric aliphatic $-CH_2$ group of 3-MPA was observed at 2851 cm^{-1} and 2922 cm^{-1}, respectively. Thiol group (-SH) stretching band was observed extremely low intensity at 2495 cm^{-1} due to the low abundance residue of unreacted -SH group of 3-MPA. Therefore, the results clearly indicate that

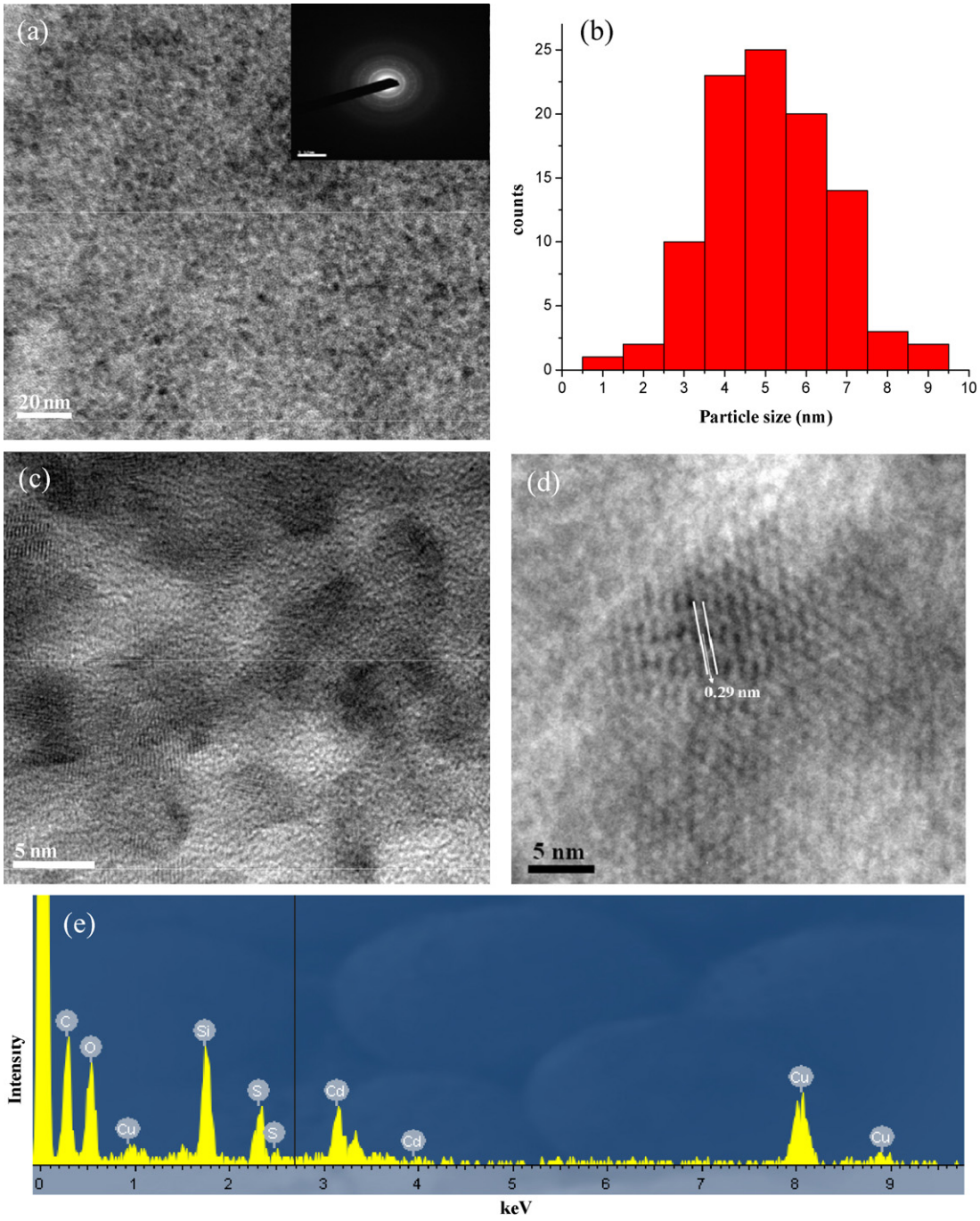

Fig. 1. HR-TEM images of CdS QDs (a) at 20 nm and (b) histograms of CdS QDs. HR-TEM images of CdS QDs (c) at 5 nm diameter and (d) amplified image of CdS QDs. The fringes at a higher magnification as shown in the inset indicate that CdS QDs are crystalline. (e) The energy-dispersive X-ray spectrum (EDXS) of CdS QDs with a spot size of 5.0 nm.

the 3-MPA was successfully capped onto the surfaces of CdS QDs.

3.2. Characterization of CdS QDs with TEM and SEM

The size and morphology of CdS QDs was investigated using a high resolution-TEM and SEM. HR-TEM provides for the study of structural composition and size distribution in CdS QDs. Fig. 1a represents the TEM image of CdS QDs at 20 nm and selected area electron diffraction. Fig. 1b reveals that size distributions of CdS QDs at 1–9 nm (~5 nm). HR-TEM image of CdS QDs at 5 nm and amplified image of single CdS QD are shown in Fig. 1c and d. The above results indicate that the quantum dots are well dispersed in the solution. The elemental composition of CdS QDs was identified by energy-dispersive X-ray spectroscopy (EDXS). Fig. 1e represents that the elemental signals of Cd, S, C and O, which are present in CdS QDs. Moreover, the signal of Cu was also found in EDX spectrum due to TEM sample holder (grid), respectively.

SEM images and EDXS of CdS QDs are shown in Supporting Information of Figure S4. SEM images of CdS QDs at low and high amplifications are depicted in Figure S4a-b of Supporting Information. These results indicate that the formed CdS QDs spheres had a “grape-bunch”- like morphology. EDXS of CdS QDs confirms that the 3-MPA was successfully coupled with the surfaces of CdS QDs

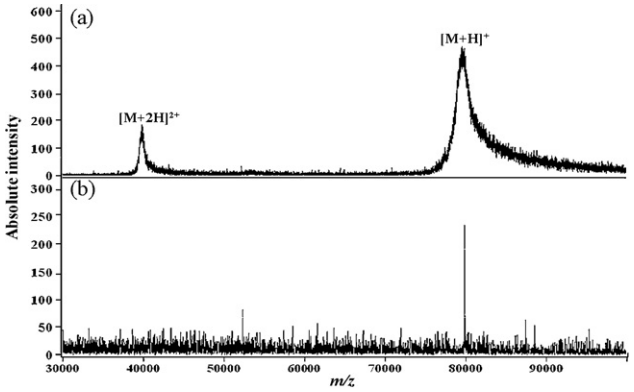

Fig. 2. LDI-TOF mass spectra of transferrin using (a) SA and (b) CdS QDs as the matrices. The mass spectra were generated by applying laser fluence at 46 μJ for SA and 89 μJ for CdS QDs. Transferrin concentration is 3.8×10^{-6} M for SA and 6.5×10^{-6} M for CdS QDs.

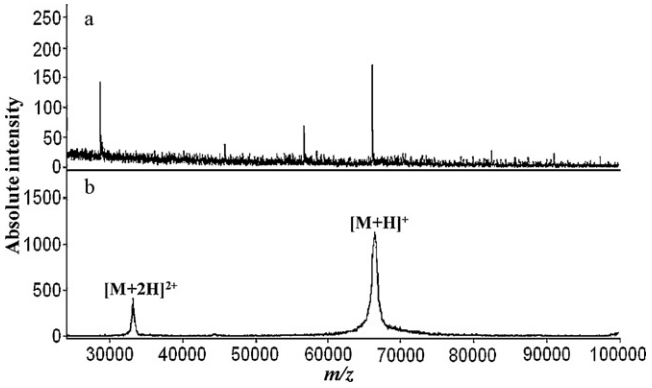

Fig. 4. LDI-TOF mass spectra of HSA using (a) CdS QDs and (b) SA as the matrices. The mass spectra were generated by applying laser fluence at 50 μJ for SA and 89 μJ for CdS QDs. HSA concentration is 3.8×10^{-6} M for SA and 7.6×10^{-6} M for CdS QDs.

(Figure S4c of Supporting Information). The above results indicate that the CdS QDs have exhibited high surface area to volume ratio and this feature is more beneficial for specific interaction of CdS QDs with biomolecules.

3.3. Analysis of large proteins with high mass resolution using CdS QDs as the matrix

The CdS QDs are applied as matrix for the analysis of large proteins (insulin, ribonuclease A, trypsin, trypsinogen, BSA, HSA, and transferrin) by LDI-TOF-MS. The obtained mass spectra of the above proteins are shown in Figs. 2–5 and Figures S5–S7 of Supporting Information. In those results, mass spectra were obtained using CdS QDs (4.4×10^{-3} M) and SA as the matrices. The mass spectra were generated by applying laser energy at 89 μJ for CdS QDs and 45–62 μJ for SA. Note that the generated mass spectra of proteins using SA as the matrix gave poor mass resolution ranging from 48 to 674 in a linear MALDI-TOF-MS (Figs. 2a, 3b, 4b, 5a and Figures S5c, S6b, S7a of Supporting Information). Interestingly, the mass peaks of the above proteins were obtained with high resolution using CdS QDs as the matrix in a linear LDI-TOF-MS (Figs. 2b, 3a, 4a, 5b and Figures S5b, S6a, S7b of Supporting Information). We observed that using CdS QDs as the matrix, analytes signal-to-noise (S/N) ratios are typically lower than using SA as the matrix (25–150 for CdS QDs and 40–220 for SA). The obtained mass peaks and mass resolutions of the proteins using CdS QDs and SA as the matrices were depicted in Table 1. These results demonstrated that the large proteins were successfully generated with high resolution

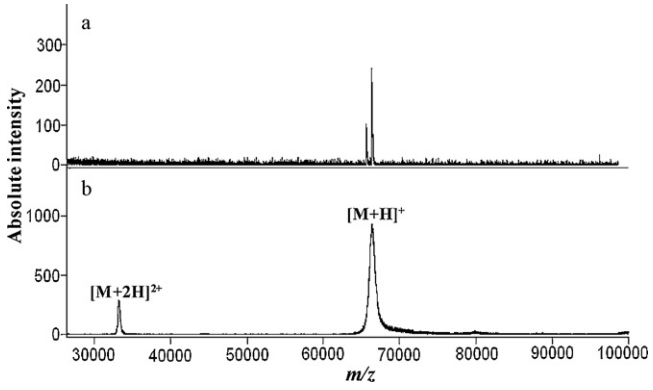

Fig. 3. LDI-TOF mass spectra of BSA using (a) CdS QDs and (b) SA as the matrices. The mass spectra were generated by applying laser fluence at 45 μJ for SA and 89 μJ for CdS QDs. BSA concentration is 3.8×10^{-6} M for SA and 7.6×10^{-6} M for CdS QDs.

at high laser energy using CdS QDs as the matrix. Generally, higher laser energies were required for the efficient desorption/ionization of analytes when using nanomaterials as matrices [30]. This can cause enhanced positive ions formation when the ablation laser is tuned to a resonant frequency that attributed to efficient gas-phase multiphoton ionization [31]. Meanwhile, laser energy is important for the formation of the analyte ions by protonation/deprotonation from collision with matrix molecules [32].

A typical example is also demonstrated in Figure S5 of Supporting Information. In Figure S5a, insulin was not well resolved by using CdS QDs as the matrix at lower laser energy (61 μJ). The reasons may be due to the following: (i) unresolved or overlapping ions ($[M+H]^+$, $[M+Na]^+$ and $[M+K]^+$) with multiplets which leads to decrease mass resolution [33]; (ii) High mass proteins typically require higher laser energy for desorption/ionization [34]. Therefore, the obtained mass peak of insulin was broad. In addition, other possibility of poor resolution for insulin may be due to instrumental reasons or overlapping masses or poor signal-to-noise [33,34]. However, at higher laser energy, CdS QDs could provide a sufficient means for desorption/ionization of proteins with narrower distribution of ion velocity which leads to higher resolution (see Figure S5b of Supporting Information). During laser desorption/ionization process, CdS QDs efficiently absorbed UV laser energy from laser, where electrons in CdS QDs can be excited from valence band to conduction band. In this process, the electrons rapidly released heat energy to proteins which results in an efficient desorption/ionization of proteins into gas phase for MS

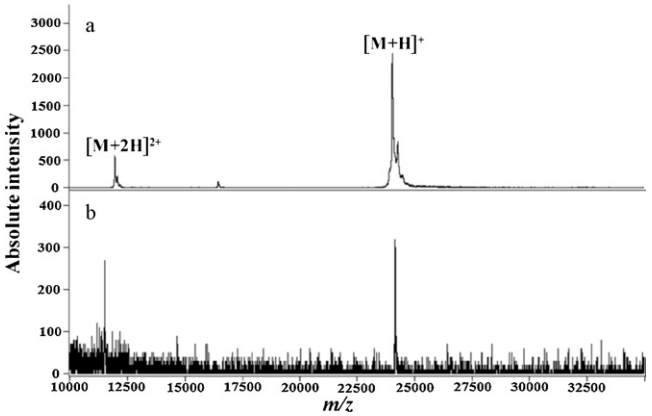

Fig. 5. LDI-TOF mass spectra of trypsinogen using (a) SA and (b) CdS QDs as the matrices. The mass spectra were generated by applying laser fluence at 57 μJ for SA and 89 μJ for CdS QDs. Trypsinogen concentration is 1.0×10^{-5} M for SA and 2.0×10^{-5} M for CdS QDs.

Table 1
Comparison of CdS QDs and SA as the matrices for the analysis of proteins in MALDI-TOF-MS.

Name of the protein	CdS QDs as the matrix			SA as the matrix		
	m/z	FWHM[a]	Mass resolution[b]	*m/z*	FWHM[a]	Mass resolution[b]
Trypsin	23607.2	9.8	2418	23588.9	50.2	464
BSA	66082.9	15.1	3025	66078.3	897	21.8
HSA	66047.1	12.4	2308	67072.2	954	28.8
Transferrin	79893.1	10.1	2107	79895.7	2500	8.2
Trypsinogen	23969.9	11.3	2089	23934.3	54.0	440
Ribonuclease A	13688.0	11.1	1220	13688.0	20.3	675
Insulin	5731.7	22.6	768	5731.3	23.4	879

[a] FWHM represents "full width at half maximum amplitude".
[b] Mass resolution is $m/\Delta m$; m is the mass of the analyte and Δm is full peak width that can measure at one-half peak's maximum height.

analysis. Also, the nanomaterials can perform efficient electron-transfer reactions [22]. Therefore, we suspect that the CdS QDs can efficiently absorb UV laser energy to generate large amount of heat for the rapid desorption/ionization of proteins with narrower distribution of ion velocity. Hence, the mass resolution of proteins was greatly improved using CdS QDs as the matrix in LDI-MS.

The mass calibration was performed by using trypsinogen and BSA with SA (Figure S8 of Supporting Information). This mass spectrum was acquired from five different sample locations on the laser target plates. The obtained mass peaks at *m/z* 23835.1 for trypsinogen and 66852.3 for BSA using SA as the matrix, respectively. The mass error of the detected analytes increases when increasing the mass of analytes (>30,000). This is due to asymmetric isotopic distribution of atoms or uncertainty in molecular weights of proteins. The mass calibrations of proteins are shown in Table S1 of Supporting Information. The limits of detection (S/N = 3) were found to be 0.80–2.0 μM for the above proteins (Table S2 of Supporting Information). The enhancement of mass resolution is especially notable for large proteins such as BSA, HSA and transferrin (~34–49 times) when compared with SA as the matrix. Next, we also found that the doubly charged ions of large proteins (5000–80,000 Da) could not be observed when using CdS QDs as the matrix in the LDI-TOF-MS which were different from those spectra obtained using SA as the matrix (Figs. 2, 4, 5 and Figures S6 of Supporting Information). This phenomenon again confirmed that the formation mechanism for the high resolution of large proteins is not conventional proton transfer which could easily produce doubly charged ions $(M+2H)^{2+}$. In addition, in the current approach, we may frequently observe fragment ions of large proteins (Figs. 4a, 5b) which were produced from high laser energy while comparing with the conventional MALDI-MS, these fragment ions were not observed. Note that when a biomolecule is placed on stub along with inorganic matrices, there is an intermediate shift in flight geometry due to finite thickness of biomolecules that result in a shift in the mass scale and un-uniform fragmentation at higher laser energy [30,35]. Therefore, the appeared lower mass peaks were not doubly charged ions (Figs. Fig 44a, Fig 55b). The upper mass limit of the present method was compared with the reported methods (Table 2). Surprisingly, when using CdS QDs as the matrix, the mass resolution of insulin was 1.7 times less than our previous report on using CdSe QDs as the matrix [36]. However, it can be noticed that the mass resolutions of the large proteins were much higher when using CdS QDs as the matrix than those of using SA as the conventional matrix. The results demonstrated that the current approach proves the excellent capability for the detection of large proteins (5–80 kDa) with high resolution (Fig. 2).

Table 2
Comparison of the present method for upper mass limit with the reported methods.

Name of the matrix	Name of the protein	Upper mass limit (kDa)	References
Fe_3O_4 NPs	Bradykinin	1.06	[18]
	Melittin	2.8	
	Insulin	5.7	
	Ubiquitin	8.5	
	Cytochrome *c*	12.2	
	Myoglobin	16.9	
Au NPs	Insulin	5.7	[20]
Au-ATP	Cytochrome *c*	12	[25]
Titania nanotube array	Carbonic anhydrase	29	[27]
Titania sol-gels	Trypsinogen	24	
Graphite	Cytochrome *c*	12	
Porous silicon chips	Insulin	5.7	
ZnS-MPA	Insulin	5.7	[28]
	Ubiquitin	8.5	
CdSe QDs	Insulin	5.7	[36]
	Lysozyme	14.5	
	Myoglobin	16.9	
Ag NPs	Bradykinin	1.06	[37]
	Angiotensin I	1.2	
CdS QDs	Insulin	5.7	Present work
	Ribonuclease A	13.6	
	Trypsin	23.6	
	Trypsinogen	23.9	
	Transferrin	79.8	
	HSA	66.0	
	BSA	66.0	

3.4. CdS QDs as the matrix for background-free detection of peptides

Next, we also investigated CdS QDs as the matrix for analysis of small molecules (peptides) such as gramicidin D (Fig. 6b), bradykinin fragment (2–8) and substance P (Figures S9a-S10b of Supporting Information). We compared these results with

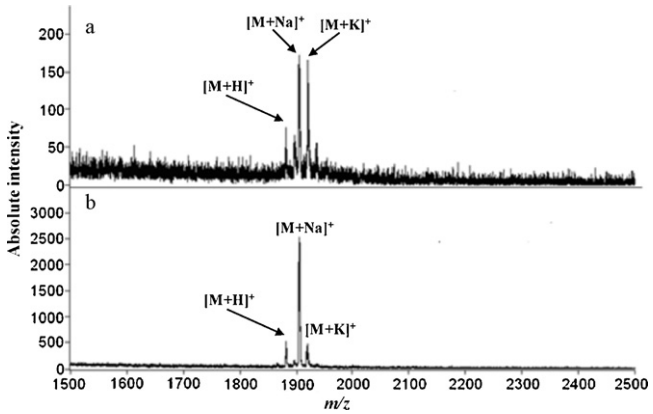

Fig. 6. LDI-TOF mass spectra of gramicidin D using (a) direct analysis without any matrix and (b) CdS QDs as the matrix. The mass spectra were generated by applying at 61 μJ of laser fluence. Gramicidin D concentration is 5.32×10^{-6} M for LDI and 2.66×10^{-6} M for CdS QDs. The mass peaks at *m/z* 1882.1, 1905.2 and 1921.3 were assigned as $[M+H]^+$, $[M+Na]^+$ and $[M+K]^+$, respectively.

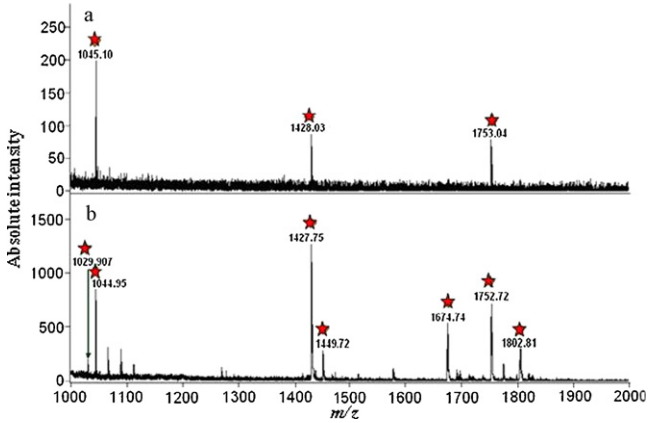

Fig. 7. MALDI-TOF mass spectra of the tryptic digest of lysozyme using (a) 2,5-DHB (130 mM) as the matrix and (b) CdS QDs as affinity probes along with 2,5-DHB as the matrix. Lysozyme concentration is 3.52×10^{-6} M. The mass peaks derived from tryptic digest of lysozyme were marked with stars.

those peptide signals obtained using LDI-MS (without any matrix) (Fig. 6a and Figures S9b and S10a of Supporting Information). The results indicated that the CdS QDs exhibit excellent capability for desorption/ionization of peptides with low background noise. The signals intensities were greatly enhanced when using CdS QDs as the matrix in LDI-MS. From mass spectra, peptide peaks of sodium ion adduct $[M+Na]^+$ at m/z 1905.5, 927.2 and 1370.5 and potassium ion adduct $[M+K]^+$ at m/z 1921.3, 943.2 and 1386.2 for gramicidin D, bradykinin fragment (1–8) and substance P, respectively. The LODs of peptides are shown in Table S2 of Supporting Information. Note that the protonated ions ($[M+H]^+$) were typically missing or with extremely low intensity and this phenomenon was similar to the results obtained for peptides using Ag NPs as the matrix in LDI-MS [37].

3.5. CdS QDs as enriching probes for tryptic digested proteins

We also demonstrated the applicability of CdS QD as affinity probes for enrichment of tryptic digest proteins such as lysozyme, myoglobin and cytochrome *c* in LDI-TOF-MS (Fig. 7, Figures S11-S12 of Supporting Information). The obtained m/z values and sequences of tryptic digested proteins are shown in Table S3–S5 of Supporting Information. Fig. 7a displays that the MALDI-TOF-MS of tryptic digest of lysozyme (3.52×10^{-6} M) by direct analysis using 2,5-DHB as the conventional matrix. Comparing this spectrum with Fig. 7b which is obtained using CdS QDs as affinity probes, the tryptic digest of lysozyme can be effectively trapped from solution. The low abundance peptides were successfully enriched with reduced background signals (5.7 folds) using CdS QDs as affinity probes. The assignments of peaks were confirmed by referring to internet (http://ca.expasy.org/). Similarly, we also applied CdS QDs as affinity probes to enrich tryptic digests of myoglobin and cytochrome *c* in LDI-MS (Figures S11b and S12b of Supporting Information). The m/z values and sequences of tryptic digested myoglobin and cytochrome *c* are depicted in Table S4–S5 of Supporting Information. Note that in the mass spectra of tryptic digested myoglobin and cytochrome *c* obtained from direct analysis (Figures S11a and S12a of Supporting Information), many unwanted mass peaks were generated by using 2,5-DHB as the matrix. Thus it might be difficult to assign mass peaks of tryptic digest proteins. However, after using CdS QDs as affinity probes for the tryptic digests of myoglobin and cytochrome *c*, the ion signals were effectively enhanced with free background interferences. This reason is CdS QDs have high surface area and affinity to bind with the tryptic digested proteins at which the desorption/ionization occurred. Meanwhile, CdS QDs-conjugated digest proteins were mixed with 2,5-DHB to facilitate crystallization. Therefore, these characteristics efficiently enhanced the tryptic digested proteins mass peaks with reduced background signals using CdS QDs as affinity probes in MALDI-TOF-MS. Hence, the CdS QDs show a notable advance in the development of matrix-free and affinity based mass spectrometric methods which is well suited for analysis of biomolecules over a wide mass range with improved mass resolution.

4. Conclusions

We have successfully demonstrated that the CdS QDs acted as an efficient matrix and as affinity probes for the desorption/ionization of proteins, peptides and tryptic digest proteins in LDI-TOF-MS without any proton source. High mass proteins such as BSA, HSA and transferrin have gained 34–49-fold improvement in mass resolution compared with traditional MALDI-MS. The CdS QDs represent a promising substitute for the matrix-free detection of large biomolecules in LDI-MS. Therefore, the CdS QDs reveal a suitable platform in LDI-MS analysis that provides for the analysis of large biomolecules with improved mass resolution.

Acknowledgement

We thank the National Science Council, Taiwan for financial support at the contract number of NSC 98-2113-M110-019-MY3.

Appendix A. Supplementary data

Supplementary data associated with this article can be found, in the online version, at doi:10.1016/j.talanta.2010.09.003.

References

[1] L.F. Marvin, A.R. Roberts, L.B. Fay, Clin. Chim. Acta 337 (2003) 11–21.
[2] C. Pan, S. Xu, H. Zhou, Y. Fu, M. Ye, H. Zou, Anal. Bioanal. Chem. 387 (2007) 193–204.
[3] O.V. Salata, J. Nanobiotech. 2 (2004) 1–6.
[4] R.S. Molday, D. MacKenzie, J. Immunol. Methods 52 (1982) 353–367.
[5] M.P. Bruchez, M. Moronne, P. Gin, S. Weiss, A.P. Alivisatos, Science 281 (1998) 2013–2016.
[6] W.C.W. Chan, S. Nie, Science 281 (1998) 2016–2018.
[7] K. Tanaka, H. Waki, Y. Ido, S. Akita, Y. Yoshida, T. Yoshida, Rapid Commun. Mass Spectrom. 2 (1988) 151–153.
[8] M. Karas, F. Hillenkamp, Anal. Chem. 60 (1988) 2299–2301.
[9] H.F. Alomirah, I. Ali, Y. Konishi, J. Chromatogr. A 893 (2000) 1–21.
[10] T. Kurihara, J.Z. Min, T. Koyooka, S. Inagaki, Anal. Chem. 79 (2007) 8694–8698.
[11] W.Y. Chen, Y.C. Chen, Anal. Chem. 79 (2007) 8061–8066.
[12] S. Trimpin, D.E. Clemmer, C.N. McEwen, J. Am. Soc. Mass Spectrom. 18 (2007) 1967–1972.
[13] M. Kussmann, M. Affolter, K. Nagy, B. Holst, L.B. Fay, Mass Spectrom. Rev. 26 (2007) 727–760.
[14] J. Wei, J.M. Buriak, G. Siuzdak, Nature 399 (1999) 243–246.
[15] Z. Shen, J.J. Thomas, C. Averbuj, K.M. Broo, M. Engelhard, J.E. Crowell, M.G. Finn, G. Siuzdak, Anal. Chem. 73 (2001) 612–619.
[16] S.F. Ren, Y.I. Guo, Rapid Commun. Mass Spectrom. 19 (2005) 255–260.
[17] H.J. Kim, J.K. Lee, S.J. Park, H.W. Ro, D.Y. Yoon, Anal. Chem. 72 (2000) 5673–5678.
[18] W.Y. Chen, Y.C. Chen, Anal. Bioanal. Chem. 386 (2006) 699–704.
[19] Y.F. Huang, H.T. Chang, Anal. Chem. 78 (2006) 1485–1493.
[20] J.A. McLean, A.K. Stumpo, H.D. Russell, J. Am. Chem. Soc. 127 (2005) 5304–5305.
[21] C.T. Chen, Y.C. Chen, Anal. Chem. 76 (2004) 1453–1457.
[22] H. Bi, L. Qiao, J.M. Busnel, V. Devaud, B. Liu, H.H. Girault, Anal. Chem. 81 (2009) 1177–1183.
[23] L. Qiao, C. Roussel, J. Wan, J. Kong, P. Yang, H.H. Girault, B. Liu, Angew. Chem. Int. Ed. 47 (2008) 2646–2648.
[24] L. Qiao, H. Bi, J.M. Busnel, J. Waser, P. Yang, H.H. Girault, B. Liu, Chem. Eur. J. 15 (2009) 6711–6717.
[25] E.T. Castellana, D.H. Russell, Nano Lett. 7 (2007) 3023–3025.
[26] D.S. Sherrod, J.A. Diaz, K.W. Russell, S.P. Cremer, H.D. Russell, Anal. Chem. 80 (2008) 6796–6799.
[27] C.Y. Lo, J.Y. Lin, W.Y. Chen, C.T. Chen, Y.C. Chen, J. Am. Soc. Mass Spectrom. 19 (2008) 1014–1020.
[28] S.K. Kailasa, K. Kiran, H.F. Wu, Anal. Chem. 80 (2008) 9681–9688.

[29] H. Li, W.Y. Shih, W.H. Shih, Ind. Eng. Chem. Res. 46 (2007) 2013–2019.
[30] F. Hillenkamp, J. Peter-Katalinic, MALDI MS: A Practical Guide to Instrumentation Methods and Applications, Wiley-VCH Verlag GmbH & Co. KGaA, Weinheim, 2007.
[31] R. Zenobi, R. Knochenmuss, Mass Spectrom. Rev. 17 (1998) 337–366.
[32] Y. Kong, Y. Zhu, J.Y. Zhang, Rapid Commun. Mass Spectrom. 15 (2001) 57–64.
[33] D.H. Russell, R.D. Edmondson, J. Mass Spectrom. 32 (1997) 263–276.
[34] J.A. Blackledge, J.A. Alexander, Anal. Chem. 67 (1995) 843–848.
[35] H.J. Griesser, K. Peter, S.L. McArthur, K.M. McLean, G.R. Kinsel, R.B. Timmons, Biomaterials 25 (2004) 4861–4875.
[36] K. Shrivas, S.K. Kailasa, H.F. Wu, Proteomics 9 (2009) 2656–2667.
[37] H. Lin, J. Chen, L. Ge, S.N. Tan, J. Nanopart. Res. 9 (2007) 1133–1138.